Applying Compactness Constraints To Seismic Traveltime Tomography

J.B. Ajo-Franklin,
Earth Resources Laboratory
Dept. of Earth, Atmospheric, and Planetary Sciences
Massachusetts Institute of Technology
Cambridge, MA 02142

B.J. Minsley,
Earth Resources Laboratory

T.M. Daley,
Earth Science Division,
Lawrence Berkeley National Laboratory, CA, USA

May 14, 2006

Abstract

Tomographic imaging problems are typically ill-posed and often require the use of regularization techniques to guarantee a stable solution. Minimization of a weighted norm of model length is one commonly used secondary constraint. Tikhonov methods exploit low-order differential operators to select for solutions that are small, flat, or smooth in one or more dimensions. This class of regularizing functionals may not always be appropriate, particularly in cases where the anomaly being imaged is generated by a non-smooth spatial process. Timelapse imaging of flow-induced seismic velocity anomalies is one such case; flow features are often characterized by spatial compactness or connectivity. We develop a traveltime tomography algorithm which selects for compact solutions through application of model-space iteratively reweighted least squares. Our technique is an adaptation of minimum support regularization methods previously developed within the potential theory community. We emphasize the application of compactness constraints to timelapse datasets differenced in the data domain, a process which allows recovery of compact perturbations in model properties. We test our inversion algorithm on a simple synthetic dataset generated using a velocity model with several localized velocity anomalies. We then demonstrate the efficacy of the algorithm on a CO_2 sequestration monitoring dataset acquired at the Frio pilot site. In both cases, the addition of compactness constraints improves image quality by reducing spatial smearing due to limited angular aperture in the acquisition geometry.

1 Introduction

The inversion of geophysical data, and tomographic imaging problems in particular, are often both non-unique and ill-posed. When confronted with a multitude of valid answers, all sensitive to small variations in noise, secondary constraints can be added to stabilize the solution and select for models which fulfill an independent notion of what a "good" model should look like. Regularization techniques accomplish both goals by minimizing a weighted seminorm of solution length in addition to fitting the data. One such approach, originally developed by *Tikhonov and Arsenin* (1977), minimizes one or more low order (0th, 1st or 2nd) spatial derivatives of the model to help choose small, flat or smooth solutions. Despite the fact

that neither flatness nor smoothness are intrinsic properties of the earth, Tikhonov methods have enjoyed remarkable success and are routinely applied to a wide range of parameter estimation problems (*Aster et al.*, 2005).

We advocate the selection of regularization operators which incorporate some notion of the physics responsible for observed property variations *e.g.* subsurface flow, thermal diffusion, fracture propagation, or sediment deposition. Due to the complexity of these processes, heuristic constraints which select for models with related characteristics might be appropriate. Since flow processes tend to localize in zones of high permeability, regularization operators favoring compact or connected anomalies seem reasonable. The infiltration of dense non-aqueous contaminants (*Kueper et al.*, 1993) and the transport of saline tracers through permeable fractures (*Day-Lewis et al.*, 2003) are two examples of compact flow features amenable to geophysical imaging.

Compact body inversion, as developed by *Last and Kubik* (1983) and more recently explored by *Portniaguine and Zhdanov* (1999), is one approach used in the potential field community for selecting compact models while still satisfying data misfit constraints. In this case, compactness implies a solution which minimizes the area of a anomaly in 2D or the volume of an anomaly in 3D. Such compactness constraints are non-linear and require the use of model-space iteratively reweighted least squares (IRLS) for effective solution. IRLS techniques are more commonly used in the data domain to solve inverse problems in the l^p norm for $1 \leq p \leq 2$ (*Bube and Langan*, 1997) but can be easily adapted to model-space reweighting (*Farquharson and Oldenburg*, 1998). Seismic traveltime tomography, a technique with demonstrated utility in a monitoring context (*Lazaratos and Marion*, 1997), is one of many geophysical inverse problems which might benefit from the incorporation of compactness constraints In this document, we will pose the traveltime tomography problem in the formalism of *Last and Kubik* (1983) and demonstrate the resulting algorithm on both a synthetic test problem and on a crosswell seismic monitoring dataset acquired at the Frio pilot sequestration site.

1.1 Principles & Theory

We initially consider the general linear inverse problem where a linear operator, $\mathbf{G}$, maps a model ($\mathbf{m}$) to a dataset ($\mathbf{d}$) i.e. $\mathbf{G}\,\mathbf{m} = \mathbf{d}$. Traditional Tikhonov regularization selects solutions that minimize an objective function combining a measure of L2 data misfit and a weighted seminorm of model length,

$$\Phi(\mathbf{m}) = \|\mathbf{G}\,\mathbf{m} - \mathbf{d}\|_2^2 + \lambda^2 \|\mathbf{W}\,\mathbf{m}\|_2^2 \tag{1}$$

where $\mathbf{W}$ is typically either $\mathbf{I}$ or a low order differential operator and λ, referred to as the regularization parameter, allows the weight given to solution length to vary. When $\mathbf{W}$ is a 1st spatial derivative operator, bias is given towards flat models while use of a laplacian favors smooth models. Minimizing equation 1 results in an augmented least-squares problem of the form,

$$\begin{bmatrix} \mathbf{G} \\ \lambda\mathbf{W} \end{bmatrix} \mathbf{m} = \begin{bmatrix} \mathbf{d} \\ 0 \end{bmatrix}. \tag{2}$$

While Tikhonov schemes have enjoyed successful application in many fields, as mentioned previously they rely on a somewhat arbitrary choice of prior structure to stabilize the inversion problem. *Last and Kubik* (1983) developed an alternative regularization strategy which selects for models with causative bodies of minimum area in addition to fitting the data. A key aspect of such a strategy is a consistent definition of area in the context of imaged anomalies. *Last and Kubik* (1983) introduced an area metric, $A(\mathbf{m})$, for n elements of constant size which can be written as,

$$A(\mathbf{m}) = a_e \lim_{\beta \to 0} \sum_{i=1}^{n} \frac{m_i^2}{m_i^2 + \beta} \tag{3}$$

where a_e is the area of a single element, m_i is the ith model parameter, and β is a factor to remove the singularity in cases where $m_i \to 0$. In the limit of small β, the interior of the right hand side of equation 3

evaluates to 0 for cases where $m_i = 0$ and 1 for non-zero values. Equation 3 can thus be viewed as a sum of binary values, each indicating whether or not a model element is "on" or "off". This definition of area leads to a joint objective function of the form,

$$\Phi(\mathbf{m}) = \|\mathbf{G}\,\mathbf{m} - \mathbf{d}\|_2^2 + \lambda^2 \sum_{i=1}^{n} \frac{m_i^2}{m_i^2 + \beta^2} \tag{4}$$

where λ integrates both model element area and a secondary regularization parameter controlling the relative weighting of the two terms. Minimization of this objective function yields a least-squares problem of the same form as equation 1 with the exception that the weighting matrix is now dependent on a model estimate,

$$\begin{bmatrix} \mathbf{G} \\ \lambda \mathbf{W}_c(\mathbf{m}) \end{bmatrix} \mathbf{m} = \begin{bmatrix} \mathbf{d} \\ 0 \end{bmatrix}. \tag{5}$$

where $\mathbf{W}_c(\mathbf{m})$ is a new diagonal matrix incorporating compactness. $\mathbf{W}_c$ can be written in explicit indicial form as,

$$W_{c_{ii}} = \left[m_{ii}^2 + \beta^2\right]^{-1/2}. \tag{6}$$

Since $\mathbf{W}_c$ is now dependent on $\mathbf{m}$, the resulting problem is non-linear and we must resort to iterative techniques, in this case a modified form of the iteratively reweighted least-squares (IRLS) method. Starting with a prior estimate of the model, equation 5 is solved for a new $\mathbf{m}$ followed by an update to the regularization operator. This solve/update sequence is repeated until a convergence criterion is met; in our implementation we use a bound (α) on the change in the area metric between non-linear iterations to terminate the procedure, $\|A(\mathbf{m}^j) - A(\mathbf{m}^{j-1})\| \leq \alpha$.

For the initial model estimate, we choose a smooth solution generated using standard regularization methods. At any given step, $\mathbf{W}_c$ should be viewed as a spatially variable damping matrix with high values in regions where the prior model estimate has a small absolute magnitude. In practice, β serves to bound the maximum value of any element in $\mathbf{W}_c$; as $m_i \rightarrow 0$, $W_{ii} \rightarrow 1/\beta$.

As is the case with many regularized inverse problems, the solution is sensitive to the choice of λ and β. *Zhdanov and Tolstaya* (2004) advocate the use of a procedure similar to the L-curve technique of *Hansen* (1992) where β is chosen to be the point of maximum curvature on the trade-off curve relating β to $A(\mathbf{m})$.

1.2 Compactness And Traveltime Tomography

Our discussion of compactness so far has been general with no assumptions regarding the operation which $\mathbf{G}$ performs, the model parametrization represented by $\mathbf{m}$, or the type of data stored as $\mathbf{d}$. We will now apply our formulation to the concrete example of seismic traveltime tomography. In this case we choose $\mathbf{m}$ to be a 2D rectilinear mesh of constant slowness cells while $\mathbf{d}$ is a vector of picked first-arrival traveltimes and $\mathbf{G}$ is the ray-path matrix.

At each iterative step in the inversion, a coupled system of the form shown in equation 5 is solved using the LSQR algorithm (*Paige and Saunders*, 1982). The starting model required to compute the first weighting matrix is calculated using the same $\mathbf{G}$ but with 1st order Tikhonov regularization instead of $\mathbf{W}_c$. In cases where the dataset to be inverted is in absolute form, we calculate relative traveltimes with respect to a homogeneous background model. This procedure minimizes the area metric with respect to perturbations from the background estimate.

2 A Synthetic Test

The compactness algorithm we describe was initially tested on a synthetic crosswell dataset. Traveltimes were generated for a symmetric 40 × 40 source/receiver configuration (1600 data) using the velocity model shown in panel [A] of figure 1 with three compact perturbations. For the inversion, model estimates were

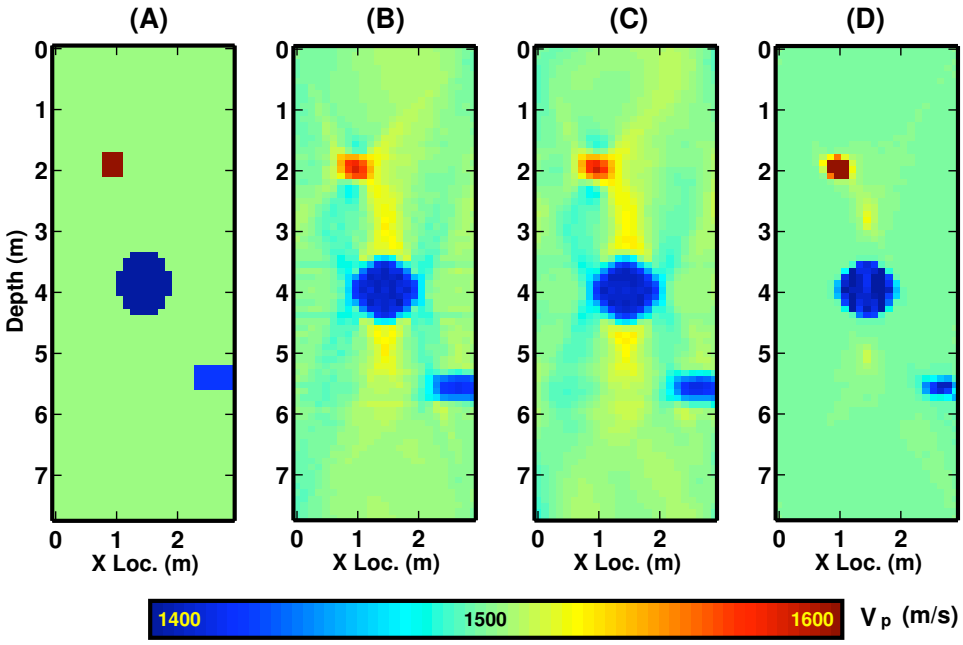

Figure 1: A noise-free synthetic test : (A) True velocity model, (B) 1st order Tikh. regularization, (C) 2nd order Tikh. regularization, (D) Compactness constraints.

calculated on a 25 × 75 sample mesh. All inversions used identical versions of the modeling operator, $\mathbf{G}$, and differ only in constraint implementation.

The right three panels of figure 1 depict noise-free inversion results using both standard 1st and 2nd order Tikhonov regularization (panels [B] and [C]) and compactness constraints (panel [D]). All three inversions exhibit similar data misfit levels. Object smearing, due to limited angular aperture, is visible in both standard tomograms. Artifacts of this type often plague traveltime imaging results and obscure both qualitative interpretation and the recovery of quantitative property estimates. As can be seen in panel [D], the addition of compactness constraints largely eliminates object smearing. The compactness inversion was initialized using an over-damped solution with 1st order Tikhonov regularization. In this case, the IRLS loop converged in only 2 IRLS iterations.

During the IRLS procedure, $\mathbf{W}_c(\mathbf{m})$ changes in accordance with variations in the previous model estimate. Examining the spatial characteristics of $\mathbf{W}_c$ provides insight into the way which the compactness constraints evolve. Figure 2 shows images of $diag[\mathbf{W}_c]$ (top row) and the corresponding estimates of $\mathbf{m}$ (bottom row) for the first two IRLS iterations. The first model estimate [A] shows the smooth over-damped starting model. The resulting $\mathbf{W}_c$ operator [B] exhibits large damping values in zones with no anomalous features and smaller values in the vicinity of the three perturbations. The second and third iterations exhibit increasingly tight constraints around the perturbed zone; this corresponds to a reduction in perturbation area, $A(m)$. Interestingly, some of the artifacts present in the starting model are still visible in later iterations except in a focused form.

Figure 3 depicts results from the same synthetic problem with the addition of 3% gaussian noise to the data. As in the noise-free case, compactness constraints minimize artifacts due to limitations in survey aperture. Additionally, image artifacts due to noise in the traveltime data are partially suppressed yielding a more interpretable image. However, the compact solution exhibits some less desirable features including a reduction in the size of the lower right velocity anomaly. Imaging artifacts above and below the central anomaly are also focused into small high amplitude features.

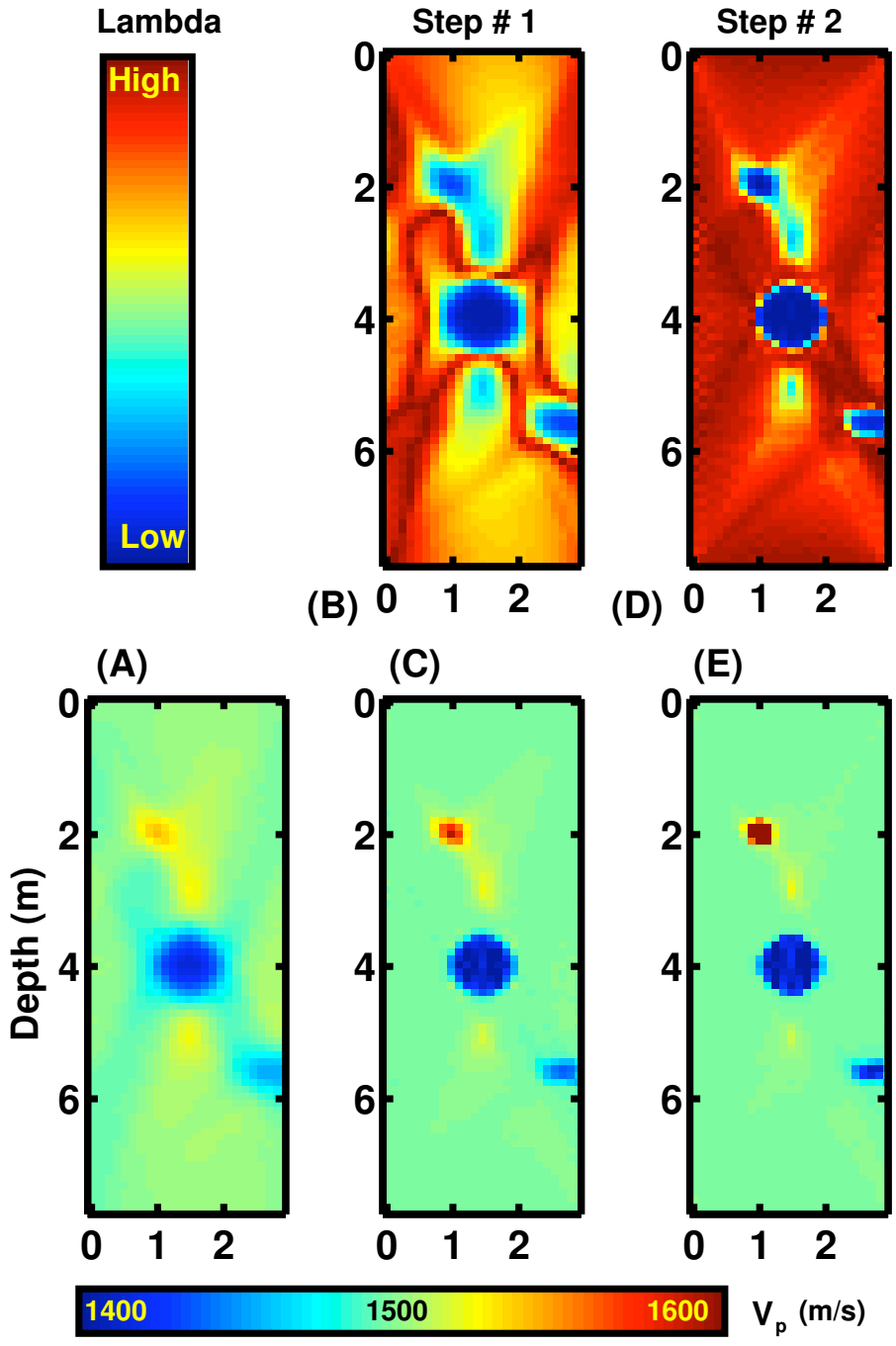

Figure 2: $\mathbf{W}_c$ and $\mathbf{m}$ as a function of iteration: The top row depicts $diag(\mathbf{W}_c)$, the spatial variations in damping. The bottom row shows the corresponding estimates of $\mathbf{m}$.

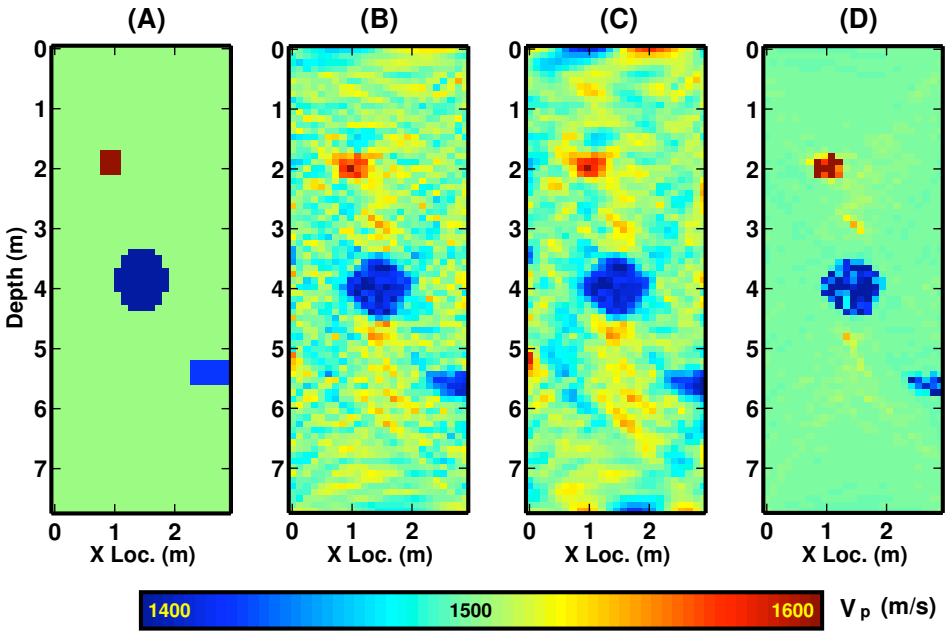

Figure 3: A synthetic test with 3% gaussian noise: (A) True velocity model, (B) 1st order Tikh. regularization, (C) 2nd order Tikh. regularization, (D) Compactness constraints.

3 Analysis Of The Frio Dataset

A complete test of the compactness algorithm was performed on a time-lapse crosswell seismic dataset acquired to monitor CO_2 sequestration at the Frio pilot site. The Frio demonstration project (*Hovorka et al.*, 2006) is an on-going multi-institution effort to improve understanding of the *in situ* dynamics of CO_2 injection within a saline aquifer located in East Texas. In the first stage of the project, 1600 $\times 10^3$ kg of supercritical CO_2 (at $P = 15$ MPa, $T = 55^oC$) was injected into a confined unit of the Frio sandstone formation; the unit, referred to as the Frio "C" sand has a dip of approximately 15 degrees. Since the supercritical phase at these P/T conditions is characterized by both a low density (≈ 700 kg/m^3 (*Hovorka et al.*, 2006)) and a low bulk modulus (≈ 0.086 GPa (*Wang and Nur*, 1989)), the zone of CO_2 saturation was expected to migrate up-dip and be visible as a zone of decreased P-wave velocity.

Motivated by previous seismic monitoring projects (*Lazaratos and Marion*, 1997) Lawrence Berkeley National Laboratory acquired two high-quality crosswell seismic datasets before and after the pilot injection in an attempt to delineate the region of subsurface CO_2 saturation. *Daley et al.* (2005) describes the data collection procedure and relevant survey parameters. Traveltimes from the baseline and repeat surveys were picked and subtracted to yield time differences (Δt). This differenced dataset was then inverted to generate a map of changes in slowness (Δs). Δs images were converted to maps of velocity changes using a background reference model obtained from logs and the baseline survey. Figure 4 shows tomography results for the Frio dataset using both standard 0th order Tikhonov regularization [panel A] and compactness constraints [panel B]. Both inversions were performed on a 60 $\times$ 200 sample rectilinear mesh. Results using 1st and 2nd order Tikhonov regularization were generally of lower quality and are not shown.

The region of injected CO_2 is visible in both images as a linear feature with decreased P-wave velocity. The dip of the imaged CO_2 zone matches prior models of local structure, increasing our confidence in the reconstruction. Both the 0th order Tikhonov and compactness constrained models exhibit a high degree of similarity within the anomalous zone. However, the addition of compactness constraints has largely eliminated artifacts related to ray coverage; these artifacts are particularly visible on the left side of the

Tikhonov solution.

The magnitude of the velocity perturbation observed in our reconstruction (≈ -800 m/s) is surprisingly large. Preliminary rock-physics analysis using poroelastic fluid substitution models similar to those used in *Nolen-Hoeksema et al.* (1995) indicate that such effects are insufficient to produce this change. Likewise, *Wang et al.* (1998) observe significantly smaller reductions in V_p during core-scale laboratory measurements of CO_2 injection. The absence of significarnt changes in V_s suggests that an increase in pore pressure can also be ruled out as a secondary factor. Future investigation is needed to identify the mechanism responsible for these large changes in rock properties.

4 Conclusion

We describe one approach for including compactness constraints in seismic traveltime tomography through use of model-space reweighting. We observe improvements in image quality in comparison to standard Tikhonov-based techniques for both a synthetic test problem and a CO_2 sequestration monitoring dataset. The strength of compactness constraints are also a weakness; in situations where the imaging target is non-compact, the size of the reconstructed feature can be inappropriately reduced. One promising extension to this approach would be to replace compactness with connectivity as a secondary constraint in the reweighting process, possibly a more effective regularization approach for flow imaging problems.

5 Acknowledgments

We would like to thank Prof. M.N. Toksöz and the Founding Members Consortium of the Earth Resources Laboratory for their generous support and guidance. Lawrence Berkeley National Laboratory collected the Frio seismic datasets with support from the U.S. Dept. of Energy's GEOSEQ program. We would also like to thank Sally Benson, Larry Myer, Susan Hovorka, the Texas Bureau of Economic Geology, and all of the contributors to the Frio project.

References

Aster, R., B. Borchers, and C. Thurber (2005), *Parameter Estimation and Inverse Problems*, Elsevier Academic Press.

Bube, K., and R. Langan (1997), Hybrid l^1/l^2 minimization with applocations to tomography, *Geophysics*, *62*, 1183–1195.

Daley, T., L. Myer, and E. Majer (2005), Acquisition of time-lapse, 6-component, P- and S-wave, crosswell seismic survey with an orbital vibrator and of time-lapse vsp for CO2 injection monitoring, in *SEG International Exposition and 75th Ann. Mtg*, Soc.Of Expl. Geophysocs.

Day-Lewis, F., J. Lane, J. Harris, and S. Gorelick (2003), Time-lapse imaging of saline tracer tests using cross-borehole radar tomography, *Water Resources Research*, *39*(10), doi:10.1029/2002WR001722.

Farquharson, C. G., and D. W. Oldenburg (1998), Non-linear inversion using general measures of data misfit and model structure, *Geophysical Journal International*, *134*, 213–227.

Hansen, P. (1992), Analysis of discrete ill-posed problems by means of the L-curve, *SIAM Review*, *34*(4), 561–580.

Hovorka, S., et al. (2006), Measuring permanence of CO_2 storage in saline formations : the Frio experiment, *Environmental Geosciences*, *13*(2), 1–17.

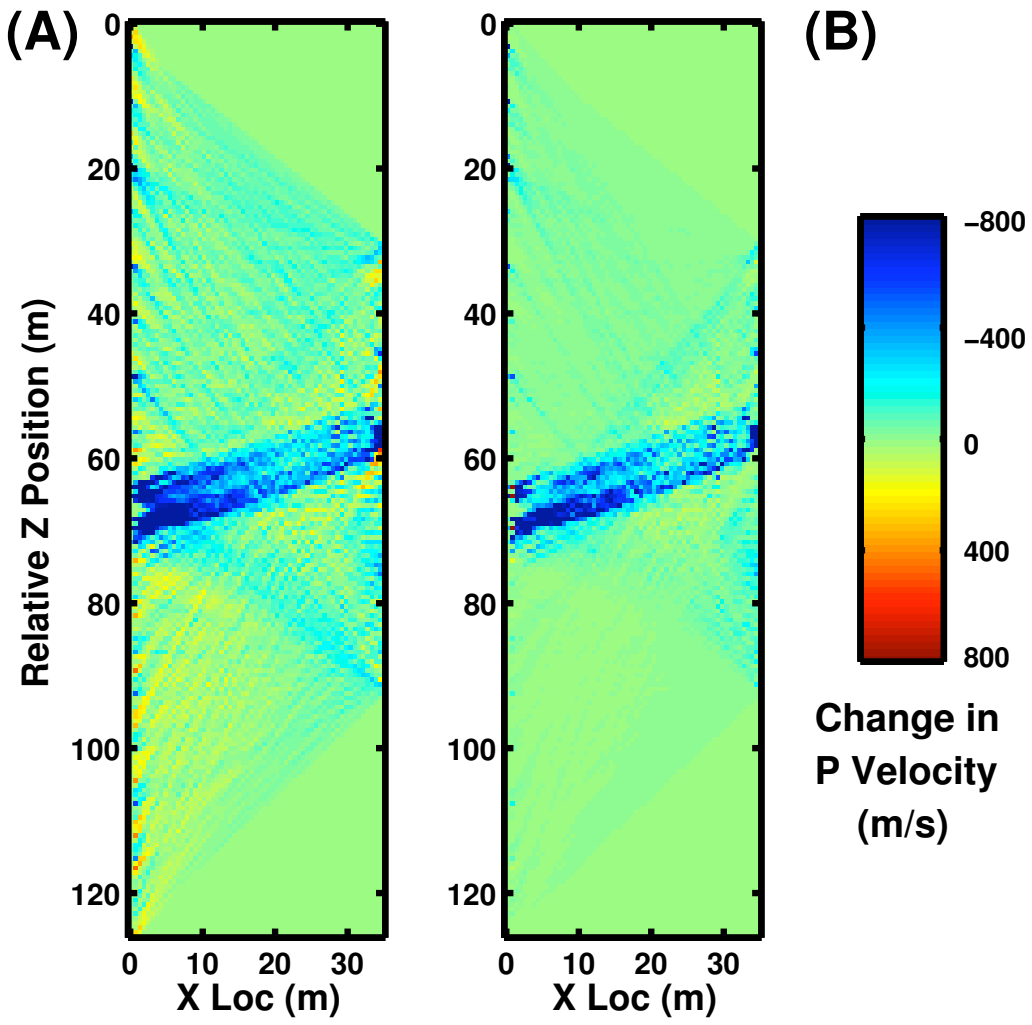

Figure 4: Results from the Frio crosswell monitoring experiment: (A) 0th order Tikh. regularization (damping), (B) Compactness constraints.

Kueper, B., D. Redman, R. Starr, S. Reitsma, and M. Mah (1993), A field experiment to study the behavior of tetrachloroethylene below the water table : Spatial distribution of residual and pooled DNAPL, *Ground Water*, *31*(5), 756–766.

Last, B., and K. Kubik (1983), Compact gravity inversion, *Geophysics*, *48*(6), 713–721.

Lazaratos, S., and B. Marion (1997), Crosswell seismic imaging of reservoir changes caused by CO_2 injection, *The Leading Edge*, *16*, 1300–1306.

Nolen-Hoeksema, R., Z. Wang, J. M. Harris, and R. T. Langan (1995), High-resolution crosswell imaging of a west Texas carbonate
reservoir: Part 5: Core analysis, *Geophysics*, *60*(3), 712–726.

Paige, C., and M. Saunders (1982), An algorithm for sparse linear equations and sparse least squares, *ACM Transactions in Mathematical Software*, *8*, 43–71.

Portniaguine, O., and M. Zhdanov (1999), Focusing geophysical inversion images, *Geophysics*, *64*(3), 874–887.

Tikhonov, A., and V. Arsenin (1977), *Solutions of Ill-posed Problems*, John-Wiley & Sons, New York, NY.

Wang, Z., and A. Nur (1989), Effects of CO_2 flooding on wave velocities in rocks with hydrocarbons, *SPE Reservoir Engineering*, *4*(4), 429–436.

Wang, Z., M. Cates, and R. Langan (1998), Seismic monitoring of a CO_2 flood in a carbonate reservoir : A rock physics study, *Geophysics*, *63*(5), 1604–1617.

Zhdanov, M., and E. Tolstaya (2004), Minimum support nonlinear parametrization in the solution of a 3D magnetotelluric invese problem, *Inverse Problems*, *20*, 937–952.